Fachtagung "Lasermethoden in der Strömungsmesstechnik"
9.–11. September 2008, Karlsruhe

SCRUTINIZING TURBULENCE CLOSURE SCHEMES FOR PREDICTING THE FLOW IN STREET CANYONS

Lars Venema[1], Dominic von Terzi[1], Christof Gromke[2] and Bodo Ruck[2]
[1] Institut für Thermische Strömungsmaschinen, Universität Karlsruhe (TH)
[2] Institut für Hydromechanik, Universität Karlsruhe (TH)

Schlagworte: Straßenschlucht, LDA-Messungen, CFD, RANS, Turbulenzmodelle
Key words: Street Canyon, LDV-Measurements, CFD, RANS, Turbulence Closure Schemes

Abstract

The flow around a street canyon was investigated by means of Computational Fluid Dynamics (CFD) and Laser Doppler Velocimetry (LDV) measurements. The Reynolds-Averaged Navier-Stokes (RANS) equations were solved with the commercial CFD tool CFX 11.0 using various turbulence models. Of special interest was the sensitivity of the CFD results to the turbulence closure schemes employed. By using the same numerical method and obtaining a grid independent solution, the performance of the RANS models was assessed. The CFD results were validated with LDV measurements.

1 Introduction

In urban areas, dispersion of traffic exhausts is a problematic issue. Especially in narrow street canyons with perpendicular approaching wind, little ventilation takes place. The outer flow is skimming over the canyon and drives a so called canyon vortex. In the literature, this phenomenon has been investigated in detail by means of wind tunnel experiments, e.g. Ahmad et al. [2005], Gromke and Ruck [2007c] and references therein. Computational Fluid Dynamics (CFD) has also been applied, but so far with limited success. A common approach in numerical simulations for this kind of flow is using the Reynolds-Averaged Navier-Stokes (RANS) equations. In particular with a $k - \varepsilon$ turbulence model, e.g. Hunter et al. [1991], Gromke and Ruck [2007b], Gromke et al. [2007] and Gromke and Ruck [2007a], to name only a few. Gromke and Ruck [2007a] compare such calculations with experimental wind tunnel data. Though qualitatively the flow field inside the canyon resembles the experiments quite well, quantitatively the numerical calculations under-estimate the velocities severely. The present study was carried out in order to determine whether these findings are due to insufficient resolution or caused by deficiencies of the turbulence modeling. To this end RANS calculations were performed with turbulence closure schemes of various sophistication level on sufficiently fine grids that ensure the elimination of any grid dependencies. In addition, the numerical results were validated with Laser Doppler Velocimetry (LDV) measurements obtained during the course of this study.

2 Experimental setup

The experiments were carried out in an atmospheric boundary layer wind tunnel, with a scale model of an isolated uniform street canyon, see figure 1. The wind flow is approaching perpendicular to the street axis with a vertical velocity profile that can be described by a power law

Grid	total # of cells	canyon cell size (m)
Coarse	4.0×10^5	6×10^{-4}
Middle	9.7×10^5	3×10^{-4}
Fine	2.2×10^6	2×10^{-4}

Table 1: Grid properties

with a profile exponent $\alpha = 0.3$. At boundary layer height, the velocity (u_δ) is 7 m/s. The height H of the buildings is 0.12 m. The canyon has a length to width ratio (L/W) of 10 and a height to width ratio (H/W) of unity. According to Hunter et al. [1991], the flow in the center of the canyon ($|y/H| < 1.5$) is then dominated by a canyon vortex and can thus be treated as a two dimensional (2D) flow field, with non-zero velocity components only in the x and z directions.

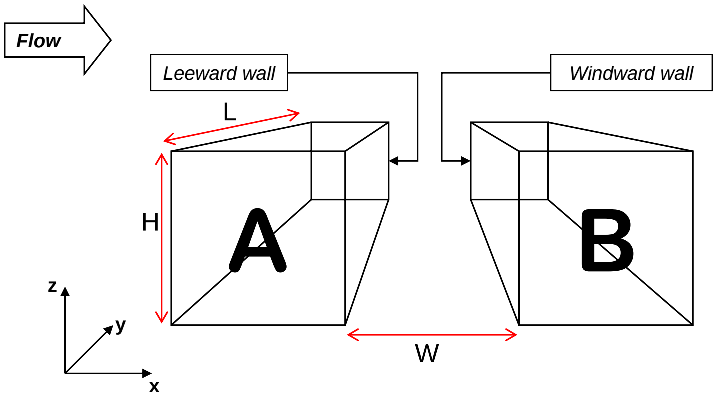

Figure 1: Street canyon geometry. The origin of the coordinate system is located at the center of the street.

The validation measurements were performed with a two-component LDV system. The seeding particles are generated by vaporising fog fluid (1,2-propanediol). The LDV measurements had a sampling frequency of 20 Hz, with a total of 1024 sampling points, so turbulence statistics could be applied. The measurement plane was located at $y/H = 0.5$. Inside the canyon only the vertical velocities could be measured due to geometrical blocking. At rooftop level, both horizontal and vertical velocity components were acquired.

3 Numerical setup

Since all measurement data were recorded within the two-dimensional flow domain, the CFD calculations were also carried out in 2D. This allows for the use of a very fine mesh, so the resolution requirements of the different closure schemes can be explored. With ICEMCFD three grids were created with increasing refinement. In each grid the area towards the street canyon is refined blockwise, with the maximum resolution being inside the canyon. In table 1 more detailed grid properties are given.

The canyon geometry is identical to the wind tunnel model. To capture the total flow field the solution domain is extended 8.3H upstream and 16.6H downstream of the canyon. The height of the domain is set to 8.3H as is the case in the wind tunnel. All surfaces are modeled by smooth no-slip walls and the inflow velocity profile is prescribed by the power law. To obtain a 2D solution, the thickness of the domain is only one cell with symmetry conditions applied in the lateral direction.

For the numerical simulations the commercial CFD code ANSYS CFX 11.0 was used, see ANSYS, Inc. [2006]. As pointed out before, the RANS equations were solved with different turbulence closure schemes. The first scheme is the well known $k - \varepsilon$ model. This scheme is a so called eddy-viscosity model, which is based on a linear relationship between the Reynolds stresses and the mean flow gradients. The turbulence is incorporated by means of a turbulent viscosity μ_t depending on the turbulent kinetic energy k and the turbulent dissipation rate ε. Both variables are calculated with the following transport equations:

$$\frac{\partial \rho k}{\partial t} + \frac{\partial \rho U_j k}{\partial x_j} = \frac{\partial}{\partial x_j}\left[\left(\mu + \frac{\mu_t}{\sigma_k}\right)\frac{\partial k}{\partial x_j}\right] + P_k - \rho\varepsilon \tag{1}$$

$$\frac{\partial \rho \varepsilon}{\partial t} + \frac{\partial \rho U_j \varepsilon}{\partial x_j} = \frac{\partial}{\partial x_j}\left[\left(\mu + \frac{\mu_t}{\sigma_\varepsilon}\right)\frac{\partial \varepsilon}{\partial x_j}\right] + \frac{\varepsilon}{k}(C_{\varepsilon 1} P_k - C_{\varepsilon 2}\rho\varepsilon) \tag{2}$$

where $C_{\varepsilon 1}$, $C_{\varepsilon 2}$, σ_k and σ_ε are constants and P_k represents the turbulence production. The turbulent viscosity is determined with

$$\mu_t = C_\mu \rho \frac{k^2}{\varepsilon} \tag{3}$$

where C_μ is also a constant. Note the lack of a wall-damping term in (2) and (3), which should be necessary for a $k - \varepsilon$ closure with wall-resolving grids.

The model is relatively easy to implement and computational inexpensive, but also has known problems. Especially in regions with sharp edges, recirculation zones are poorly predicted. Due to a stagnation point anomaly, flow separation is under-estimated. Since a typical street canyon geometry is characterized by sharp rectangular edges, the suitability of RANS calculations based on the $k - \varepsilon$ closure may be questioned.

The second turbulence closure scheme used is the Shear Stress Transport (SST) model. The SST model is based on the $k - \omega$ model, but accounts for the transport of turbulent shear stress. The over-estimation of the eddy viscosity, which is the case with the standard $k - \varepsilon$ and $k - \omega$ models, is overcome by applying a limiter to the formulation of the eddy-viscosity

$$\nu_t = \frac{a_1 k}{\max(a_1 \omega, SF)} \tag{4}$$

where $\nu_t = \mu_t/\rho$, F is a blending function to restrict the limiter to the wall boundary layer and S is an invariant measure of the strain rate. The blending function is given as

$$F = \tanh(arg^2) \quad \text{with} \quad arg = \max\left(\frac{2\sqrt{k}}{\beta' \omega y}, \frac{500\nu}{y^2 \omega}\right) \tag{5}$$

in which β' is a model constant, ω the turbulent frequency, defined as $\omega = \varepsilon / C_\mu k$ and y the distance to the nearest wall.

The last model used, is the Speziale, Sarkar, Gatski (SSG) model, a full Reynolds stress closure. All Reynolds stresses ($\overline{u_i u_j}$, six in total) are calculated by means of individual transport equations:

$$\frac{\partial}{\partial t}(\rho \overline{u_i u_j}) + \frac{\partial}{\partial x_k}(U_k \rho \overline{u_i u_j}) = P_{ij} + \phi_{ij} + \frac{\partial}{\partial x_k}\left[\left(\mu + \tfrac{2}{3} c_s \rho \frac{k^2}{\varepsilon}\right)\frac{\partial \overline{u_i u_j}}{\partial x_k}\right] - \tfrac{2}{3}\delta_{ij}\rho\varepsilon \tag{6}$$

where c_s is a model constant, P_{ij} the exact production term, ϕ_{ij} the pressure–strain rate correla-

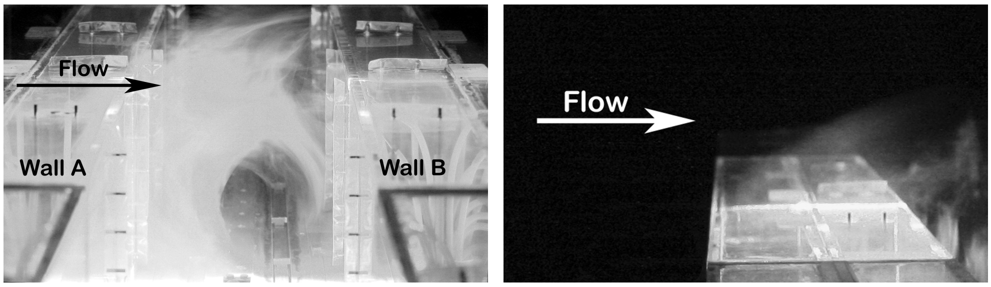

(a) Rotating canyon vortex (b) Rooftop of the windward building

Figure 2: Laser light sheet flow visualizations at the center of the street canyon

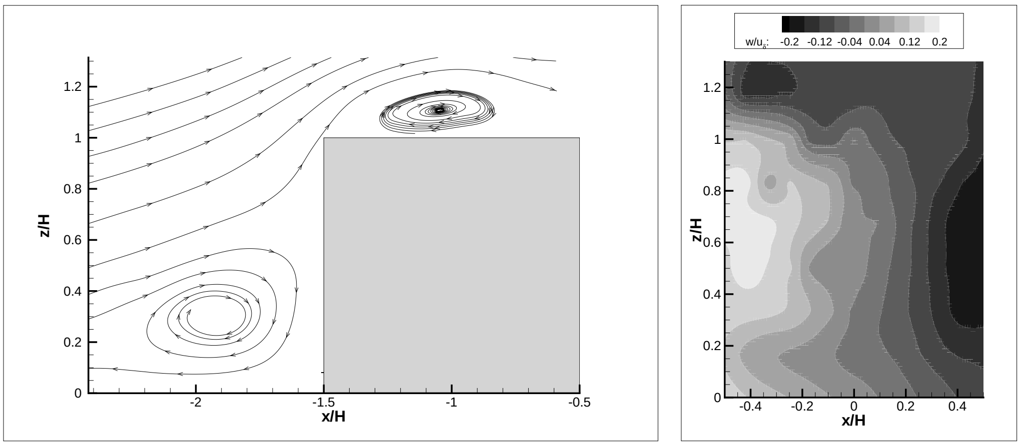

(a) Streamlines in front and on top of the windward building (b) Vertical velocity

Figure 3: Experimental results of the measured flow field around the windward building

tion and k is defined as $\frac{1}{2}\overline{u_i u_i}$. Additionally, an ε transport equation needs to be solved, see the last two terms in (6). Compared with two-equation models, five additional transport equations need to be solved. This considerably increases the complexity and cost of the calculations, but has as advantage that it does not depend on the eddy-viscosity assumption, therefore, it does not share its limitations. Moreover, the computational cost is still considerably less than in case of a so called Large–Eddy Simulation (LES), for which the time-dependent large-scale flow structures need to be resolved in all three dimensions.

4 Experimental results

The flow around the street canyon turns out to be highly intermittent. Figure 4 shows two laser sheet flow visualizations where smoke was being released inside the canyon. Clearly visible is the canyon vortex in figure 2(a). Figure 2(b) shows the canyon at another time step, displaying a totally different flow field where smoke is transported on the roof of the windward building.

In figure 3 the mean velocities scaled with u_δ are displayed. The streamlines show areas of recirculating flow in front of the windward building, the so-called bolster eddy, and on the rooftop. The vertical velocity flow field inside the canyon (scaled by u_δ) indicates the existence of a canyon vortex. This vortex rotates clockwise with a maximum speed of approximately $0.2u_\delta$ and exceeds the rooftop level to $z/H \approx 1.1$. Important for the ventilation of the street canyon is the relative strong downflow above the canyon. In particular at $x/H = -0.4$ there is a strong negative vertical velocity observed in the vicinity of $z/H = 1.2$.

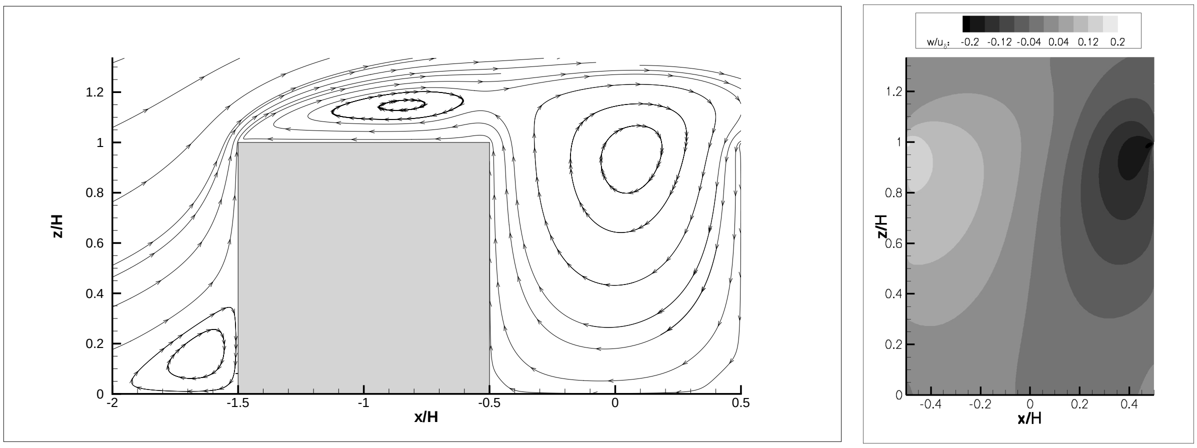

(a) Streamlines around the windward building

(b) Vertical velocity

Figure 4: Results of simulations with $k - \varepsilon$ closure; coarse grid.

5 Numerical results

Since the adequacy of the turbulence modeling is the focus of this study, it is important to eliminate other influences. The impact of the numerical method is cancelled out by using the same method for all models. Grid independency is confirmed by comparing the results of the three different grids listed in table 1. In the following sections, the results obtained with the $k - \varepsilon$, SST and SSG closure schemes will be discussed.

5.1 $k - \varepsilon$ closure

Figure 4 shows the flow field around the windward building and inside the street canyon. As the streamline plot shows, the recirculation zone on the rooftop is over-estimated, the flow does not reattach and even interacts with the canyon vortex. The bolster eddy on the windward side of the building is not as pronounced as in the experiments. Looking at the vertical velocity distribution, the results are qualitatively reasonable, though the CFD simulations do not show the downward flow above the canyon, as is seen in the experiments. Quantitatively, the velocity is severely under-estimated in a large region of the canyon.

A better quantitative view is given in figure 5. Here, the vertical velocity profile is given at three locations on the roof of the windward building: $x/H = -1.42$ is located, near the windward edge of the building, $x/H = -1.08$ is about halfway the rooftop and $x/H = -0.58$ is near the edge to the street canyon. The flow separates and reattaches on the rooftop. Since this is one of the known difficulties for turbulence models, this region is of special interest here.

As can be seen in figure 5, the solution is independent of the grid resolution. So the grid resolution requirement is met. For $z/H > 1.2$ the data fits the experimental data quite well, however, near the wall, noticeable differences occur. It is clearly visible that the recirculation zone is overestimated by the simulation. At $x/H = -0.58$, the simulated flow field exhibits a negative horizontal velocity near the wall, whereas the wind tunnel experiment shows only positive u velocities. This is surprising, since the $k - \varepsilon$ closure is known to under-estimate the recirculation zone.

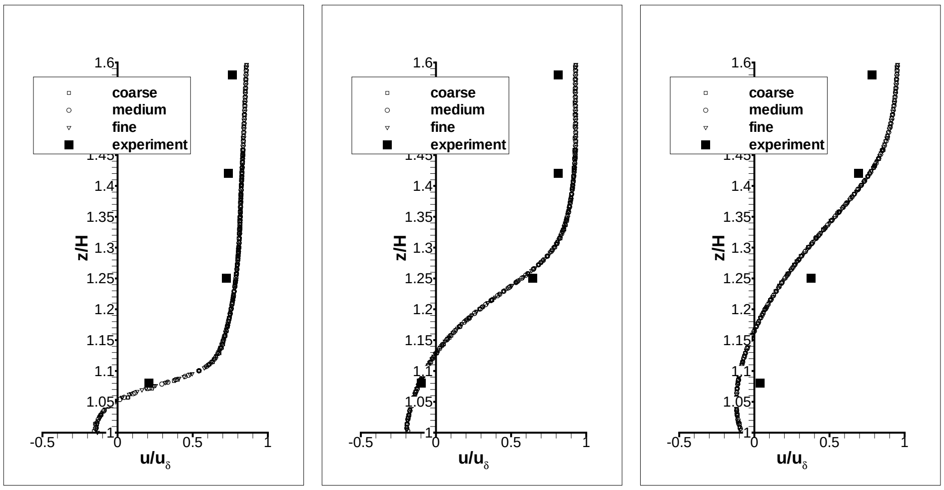

(a) $x/H = -1.42$ (b) $x/H = -1.08$ (c) $x/H = -0.58$

Figure 5: Horizontal velocity u/u_δ versus z/H on the roof of the windward building; results of simulations with the $k-\varepsilon$ model on various grids.

5.2 Shear stress transport and Reynolds stress modeling

The SST model also produces a grid-independent solution. In figure 6, the streamlines and vertical velocity contours of the coarse grid are given. Based on the experimental evidence, the bolster eddy might be captured more realistically in comparison to the $k-\varepsilon$ closure. However, around the canyon the flow field is completely different. The recirculation zone is stretched along the full length of the roof and continues above the canyon. In the canyon region, two rotating flow structures occur: a clockwise rotating flow at rooftop level and at ground level a canyon vortex rotating counter-clockwise. This is clearly not in line with the experimental data. Consequently, the vertical velocities displayed in the contour plot do not agree either. Both direction and magnitude are not in correspondence with the wind tunnel measurements.

The calculations with the SSG closure had convergence difficulties. The obtained solution is displayed in figure 7. The same effects are noted as with the SST modeling. The rooftop recirculation is too large in the flow direction and inside the canyon two counter-rotating flow structures are present. The velocities are severely under-estimated. Note that preliminary studies with grids too coarse to capture the recirculating flow on the rooftop show only one clockwise turning canyon vortex, i.e. a flow field more in agreement with the experiments.

Figure 8 compares the vertical velocity profile for all turbulence models investigated. Despite the large differences seen in the streamline plots, on the rooftop all models show qualitatively the same trend. Until $x/H = -1.08$ the fit with the experimental data is reasonable. For $x/H > -1.08$ all models over-estimate the recirculation near the rooftop. Remarkable is the fact that the calculations with the $k-\varepsilon$ closure are closest to the experimental data. Although this may well be a fortuitous case of error balancing.

6 Conclusions

In this study the simulation of street canyon flow was investigated. Since the same numerical method was used and the solutions were grid-independent, it can be concluded that the main differences between the simulations were caused by the turbulence modeling. Unfortunately none of the used turbulence closure schemes led to a fully satisfying result demonstrating

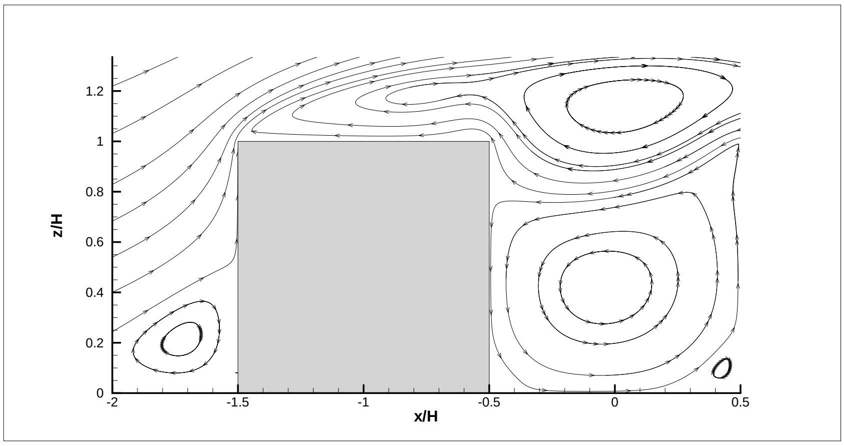

(a) Streamlines around the windward building

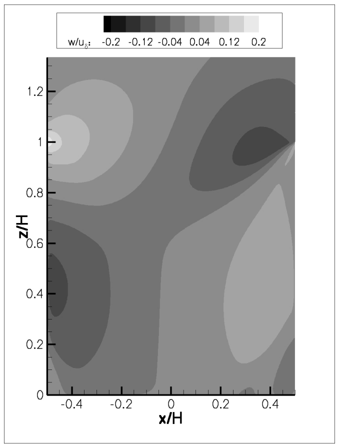

(b) Vertical velocity

Figure 6: Results of simulations with SST closure; coarse grid.

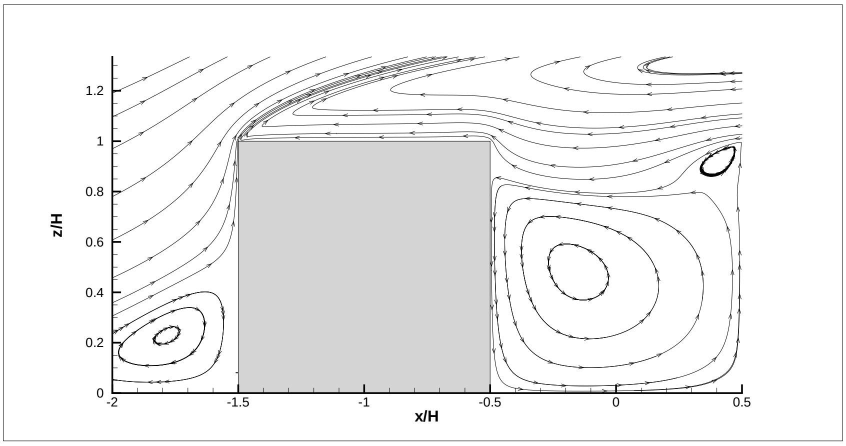

(a) Streamlines around the windward building

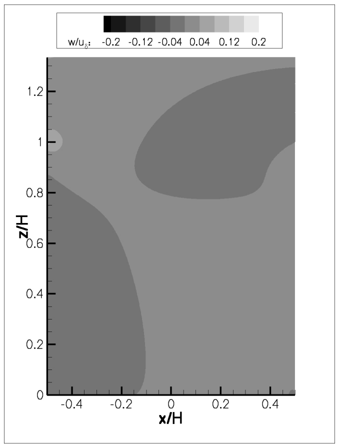

(b) Vertical velocity

Figure 7: Results of simulations with SSG closure; coarse grid.

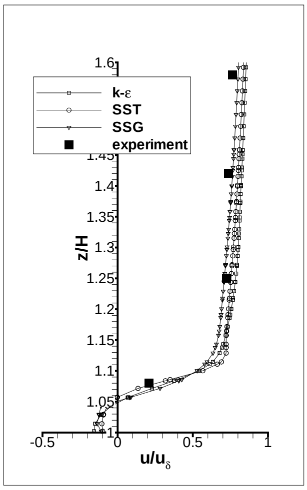

(a) $x/H = -1.42$

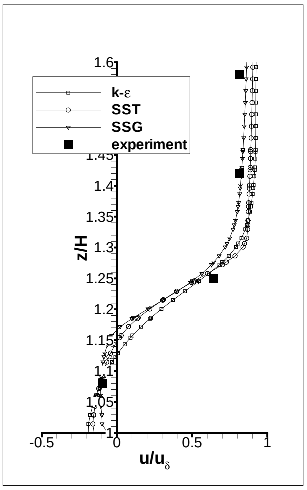

(b) $x/H = -1.08$

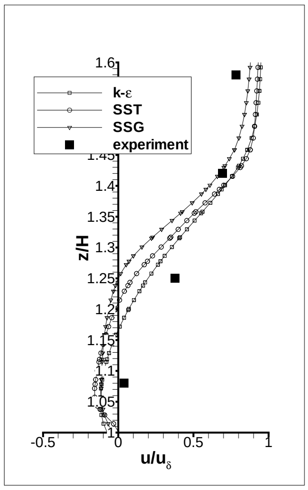

(c) $x/H = -0.58$

Figure 8: Horizontal velocity u/u_δ versus z/H on the roof of the windward building; results of simulations on a coarse grid with various turbulence closure models.

that predicting the flow in street canyons is a challenging problem for RANS calculations. The $k-\varepsilon$ model showed a qualitatively reasonable solution, but was quantitatively relative poor in comparison with the LDV measurements. Counterintuitively, the more advanced SST and SSG models did not produce better results. The rooftop recirculation zone was over-estimated severely, causing a qualitatively different flow field inside the canyon. As a consequence, one should be very careful in interpreting the results of a RANS calculation for this kind of flow. The variation of solutions between the different turbulence models is so large that there is a very high uncertainty factor.

In conclusion, we recommend that within a series of RANS parameter studies, key simulations, if possible, are either validated by means of wind tunnel experiments or LES. Alternatively, to strike a balance between inexpensive RANS calculations and high-fidelity but costly LES, it might be worthwhile to employ hybrid LES/RANS methods. Such methods have shown great promise for the simulation of complex turbulent flows, see the review of Fröhlich and von Terzi [2008]. Furthermore, some of these methods are already available in commercial CFD software.

References

K. Ahmad, M. Khare, and K. Chaudhry. Wind tunnel simulation studies on dispersion at urban street canyons and intersections - a review. *Journal of Wind Engineering and Industrial Aerodynamics*, 93:697–717, 2005.

ANSYS, Inc. *ANSYS CFX-Solver Theory Guide, Release 11.0*, 2006.

J. Fröhlich and D. von Terzi. Hybrid LES/RANS methods for the simulation of turbulent flows. *Progress in Aerospace Sciences*, 2008. doi:10.1016/j.paerosci.2008.05.001, in press.

C. Gromke and B. Ruck. Strömungsfelder in Strassenschluchten mit und ohne Baumpflanzungen - Vergleich zwischen LDA-Messungen und CFD-Simulationen. *Proc. 15. GALA Fachtagung "Lasermethoden in der Strömungsmesstechnik"*, 2007a.

C. Gromke and B. Ruck. Experimentelle und numerische Untersuchungen zur Ausbreitung von Autoabgasen in städtischen Straßenschluchten mit Baumpflanzungen. *10. Dreiländertagung der Windtechnologischen Gesellschaft*, 2007b.

C. Gromke and B. Ruck. Influence of trees on the dispersion of pollutants in an urban street canyon - experimental investigation of the flow and concentration field. *Atmospheric Environment*, 41:3287–3302, 2007c.

C. Gromke, J. A. Denev, and B. Ruck. Dispersion of traffic exhausts in urban street canyons with tree plantings - experimental and numerical investigations. *Proc. of The International Workshop on Physical Modelling of Flow and Dispersion Phenomena (PHYSMOD2007)*, 1, 2007.

L. Hunter, I. Watson, and G. Johnson. Modeling air flow regimes in urban canyons. *Energy and Buildings*, 15-16:315–324, 1991.